JOURNAL OF NEUROPHYSIOLOGY
Vol. 58, No. 5, November 1987. *Printed in U.S.A.*

Retinal W-Cell Input to the Upper Superficial Gray Layer of the Cat's Superior Colliculus: A Conduction-Velocity Analysis

DAVID M. BERSON

Section of Neurobiology, Division of Biology and Medicine, Brown University, Providence, Rhode Island 02912

SUMMARY AND CONCLUSIONS

1. I have used several methods to estimate the conduction velocities of retinal afferents innervating the upper 50–100 μm of the stratum griseum superficiale (the upper SGS). The measurements were based on a unitary extracellular potential unique to this sublamina, which was first described by McIlwain (28). He termed it the juxtazonal potential (JZP), and showed that it results when a single spike invades the terminal arbor of a single retinal afferent to the upper SGS, triggering synchronous excitatory postsynaptic potentials in postsynaptic collicular cells.

2. Individual unitary JZPs were evoked at fixed latencies by weak shocks to the optic disk, chiasm, or tract. When the same JZP could be evoked in isolation from two stimulus sites, the conduction velocity of the axon triggering the JZP was estimated by dividing the conduction time between the stimulating electrodes (i.e., the "latency difference") into the distance separating these electrodes. This "latency-difference method" lacked general utility, however, since the same JZP could only rarely be evoked in isolation from two stimulus sites.

3. This limitation was circumvented by means of a collision method. When a stimulus that evoked a JZP in isolation was preceded by a sufficiently intense conditioning shock to a second, more central stimulus site, the conditioning stimulus caused the JZP to fail in an all-or-none fashion. It was assumed that when the JZP failed, the conditioning stimulus had exceeded the spike threshold of the axon mediating the JZP and that an antidromic action potential had collided with the orthodromic spike initiated at the peripheral stimulus site. Assessment of the critical interstimulus interval for producing such a collision, together with measurements of the axon's refractory period and the interelectrode conduction distance, permitted an estimate of the conduction velocity of the JZP-triggering axon. Conduction-velocity estimates generated in this way closely matched those based on the latency-difference technique when both methods could be applied.

4. Conduction velocities of 31 JZP-triggering axons analyzed by the collision method ranged from 2.9 to 6.8 m/s [4.6 $\pm$ 1.0 (mean $\pm$ SD)]. Comparable estimates were obtained for such axons by alternative methods based on the absolute latencies of electrically evoked JZPs or of the field potential to which they contribute. The conduction velocities of JZP-triggering axons fell within the range reported for retinal W-cells and entirely outside those of X- and Y-cells, confirming earlier evidence for W-cell input to the upper SGS (7, 15, 18, 28). In addition, though, the conduction velocities of these axons were slower and more homogeneous than those of W-cells overall. Their conduction velocities were much slower on average than those reported for "tonic" W-cells, but matched quite closely those of "phasic" W-cells, particularly those with ON/OFF centers (4, 5, 49).

5. These findings, together with earlier results of others, suggest that the dense retinal input to the uppermost SGS originates predominantly in a subclass of retinal W-cells

having small somas, extremely slow axonal conduction velocities, crossed projections from both the nasal and temporal hemiretina, and phasic responses to standing contrast.

INTRODUCTION

The superficial layers of the mammalian superior colliculus represent a major component of the central visual pathways, yet their role in visual function remains obscure. Clues to the contribution of the superficial layers to vision may come from a functional analysis of their retinal inputs, since these differ sharply from those of the dorsal lateral geniculate nucleus (LGNd). In the cat, for example, retinal X-cells project heavily to the LGNd, but contribute little to the retinocollicular pathway. W-cells, on the other hand, provide most of the retinal input to the superior colliculus, but a smaller fraction of total retinogeniculate input (4, 5, 7, 8, 15, 18, 27–29, 33, 40, 56; see Refs. 35 and 47 for review).

It has been clear from the outset that W-cells form a heterogeneous class, exhibiting wide variation in receptive-field properties, somadendritic morphology, retinal distribution, axonal conduction velocity, pattern of decussation at the optic chiasm, and central terminations (4, 5, 8, 22–24, 27, 37, 38, 39, 44, 47–53, 56). Indeed, some have questioned whether W-cells constitute a meaningful class at all (5, 17, 35, 44). There is evidence to suggest that a subset of W-cells innervates the colliculus. Many of the smallest ganglion cells (somal diameters <15 μm) project to the colliculus, but few of these presumed W-cells project to any component of the LGNd complex (27, 37, 44, 52, 53, 56). By contrast, the largest of presumptive W-cells (somal diameters ~ 18–30 μm) have substantial projections to the geniculate complex, but make relatively little contribution to the retinocollicular projection (27, 37, 44, 52, 53, 56).

Evidence for functional specialization of the W-cell input to the colliculus is especially strong for the uppermost 50–100 μm of the superficial gray layer, here termed the upper SGS. This sublamina contains the vast majority of retinotectal terminals (1, 2, 10, 11, 14, 19, 30, 31, 45, 46), and these appear to arise largely or exclusively from W-cells (7, 15, 18, 28, 29) located in the contralateral eye (1, 2, 10, 11, 14, 19, 46). This dense superficial tier of retinal termination extends to the rostral pole of the colliculus (10, 14), which represents the ipsilateral visual hemifield (contralateral temporal retina; Refs. 6, 14). Thus retinal input to the upper SGS presumably arises from one or more W-cell subtypes known to emit largely or exclusively crossed projections (23, 50).

Further clues to the functional identity of W-cell afferents to the upper SGS could come from analysis of their conduction velocities, since the receptive-field properties and axonal conduction velocities of W-cells tend to be correlated (4, 5, 22, 38, 49). Unfortunately, such an analysis faces serious technical problems. Direct recordings of W-cell axons in the upper SGS appear to be ruled out by their extremely small caliber, whereas evoked responses of collicular neurons presumably reflect the convergent actions of multiple retinal and nonretinal afferents, some of which may terminate deeper in the SGS. Fortunately, an alternative approach to the problem is afforded by a physiological feature unique to the upper SGS—the "juxtazonal potential" (28).

Juxtazonal potentials (JZPs) are unitary, negative extracellular potentials of the cat's colliculus discovered in 1978 by McIlwain (28; see Fig. 1). They are so-named because they can be recorded only in a thin stratum lying just below the zonal layer of the colliculus, that is, in the upper SGS. Each JZP appears to be an extracellularly recorded compound excitatory postsynaptic potential (EPSP) that results when a single spike invades one retinal afferent arbor, producing synchronous depolarization of postsynaptic collicular elements (28). Several observations link JZPs to the retinal input to the upper SGS. The sublayer in which JZPs can be recorded corresponds closely to the stratum receiving the densest retinal input. JZPs can be evoked electrically or visually from the contralateral eye, but not from the ipsilateral eye, matching the almost exclusively crossed retinal projections to the upper SGS. Chronic ablation of the visual cortex has no apparent effect on JZPs. An intense shock to the optic pathway recruits large numbers of unitary JZPs which sum to form the well-

known negative field potential characteristic of the upper SGS. This field potential reflects the dense current sink generated by excitatory synaptic input from W-cells to the upper SGS (7, 28). Stimulation of the optic pathway drives collicular cells with direct W-cell input at latencies matching those of unitary JZPs or their associated field potential (15, 28).

Each JZP appears to be mediated by a single retinal W-cell axon (28). Individual JZPs can be evoked in all-or-none fashion by weak shocks to the optic nerve or tract. Each JZP has a fixed latency and a sharp and stable threshold (see Fig. 2). Many JZPs are preceded by a small biphasic prepotential (see Fig. 1). JZPs that exhibit such prepotentials always occur together with them, a fixed delay of roughly half a millisecond separating the two. Tetanic stimulation of retinofugal fibers rapidly reduces the amplitude of the JZP, but does not affect the prepotential, suggesting a postsynaptic origin for the JZP and a presynaptic one for the prepotential.

Thus the prepotential apparently signals the invasion of a spike into the terminal arbor of a single W-cell afferent to the upper SGS, whereas the JZP reflects the local current sink generated by the resulting synchronous depolarization of postsynaptic collicular elements. Since JZPs are easily recorded and signal the activation of single retinal afferents to the upper SGS, they offer a unique opportunity to characterize the conduction velocity of these axons. With this goal in mind, I have analyzed the latency behaviors of JZPs. The results reveal that the retinal axons innervating the upper SGS and triggering JZPs are among the most slowly conducting of any in the W-cell class. This supports the hypothesis that a functional subclass of W-cells provides the major retinal input to the cat's superior colliculus.

METHODS

Preparation

Experiments were carried out on 11 adult cats anesthetized initially with Nembutal (35 mg/kg ip) or ketamine hydrochloride (30 mg/kg ip). Animals were not paralyzed. Supplementary Nembutal or ketamine were administered intravenously as needed to suppress spontaneous organized movements of the limbs. Optimal results were obtained using Nembutal for initial anesthesia and very small doses of ketamine (less than 1 $mg \cdot kg^{-1} \cdot h^{-1}$) during recording. In a few cats, small doses of acepromazine maleate (1–2 mg, im) were given to enhance the action of the anesthetics. Salivation and respiratory secretions were controlled as necessary with atropine sulfate (0.04 mg/kg im).

Cats were placed in a stereotaxic instrument, the pupils dilated with topical atropine sulfate, nictitating membranes retracted with phenylephrine hydrochloride, and corneas kept from drying with plano contact lenses. In later experiments, a tracheotomy was performed to permit artificial respiration during brief periods of respiratory arrest that barbiturate-anesthetized cats sometimes exhibited upon initial infusion of ketamine. Portions of the skull were removed to provide access to the right superior colliculus, optic tract, and optic chiasm. The edges of the scalp were sutured to a brass ring, and the exposed brain was covered with a pool of warm mineral oil.

Electrical stimulation and recording

A concentric bipolar stimulating electrode (Rhodes NE-100) was placed in the right optic tract (OT) at Horsley-Clarke coordinates anterior 6.5–8.5 and lateral 11.0–13.0. A second such electrode was placed in the optic chiasm (OX) at coordinates anterior 13.0–14.5 and lateral 0.5–2.0. The sharpened tip of a third concentric electrode was inserted through a scleral slit into the left optic disk (OD) under ophthalmoscopic guidance. Accurate placement of these electrodes was confirmed by recording through them visually evoked activity and field potentials evoked by shocks delivered to the other stimulus sites. A stimulus isolator delivered constant-current, square-wave pulses of <5 mA through these electrodes. All stimuli were 50 μs in duration. Current strength was monitored by measuring the voltage drop across a 1,000Ω resistor in series with each electrode.

Collicular field potentials and individual juxtazonal potentials were recorded extracellularly using Insl-X coated tungsten microelectrodes (2–12 MΩ impedance at 1,000 Hz) or filament-containing glass micropipettes filled with 4M NaCl (tip diam. <1 μm; impedance 4–17 MΩ). Isolation of JZPs was generally superior with the glass electrodes, but there were no striking differences between electrode types in the waveform or latency of evoked JZPs. Electrical responses were amplified and monitored conventionally. AC recording was used throughout, and recording bandpass adjusted as necessary to optimize the signal-to-noise ratio for unitary JZPs. The low-frequency cutoff generally ranged from 1 to 300 Hz and the high-frequency cutoff from 1 to 10 kHz. Changes in recording band pass had no ap-

preciable effect on the latencies of JZPs, which were measured from the onset of the stimulus artifact to the beginning of the downstroke of the JZP. Traces of interest were stored on magnetic tape. Selected recording sites from penetrations with tungsten electrodes were marked by electrolytic lesions.

Histology and estimates of conduction distance

At the end of the experiment, animals were given a lethal dose of Nembutal and perfused through the carotids with 10% formalin. The brain and the left optic nerve and eye were removed from the skull. Axonal conduction distances separating the stimulus points in the optic disk, chiasm, and tract from one another and from the center of the colliculus were estimated by laying a thread along the optic pathway. Two to five measurements were made for each segment of the conduction route in each cat, and averages of these values were used to compute conduction distances individually for each cat.

RESULTS

With appropriate recording band pass, electrodes located immediately below the collicular surface readily recorded slow, unitary negative potentials (Fig. 1) of the sort McIlwain (28) termed JZPs. As originally reported, individual JZPs had rapid smooth downstrokes and a slower return to base line, lasting up to 5 ms or more. Juxtazonal potentials could reach several hundred microvolts in amplitude. They were sometimes preceded by a biphasic prepotential of much lower amplitude (arrows in Fig. 1). Juxtazonal potentials could be recorded only in the uppermost 100 μm or so of the superficial layers, in or near sublamina II_1 of the superficial gray (19). These potentials occurred spontaneously (Fig. 1) and could also be evoked by visual stimulation of a critical region of the visual field and by electrical stimulation of retinofugal fibers.

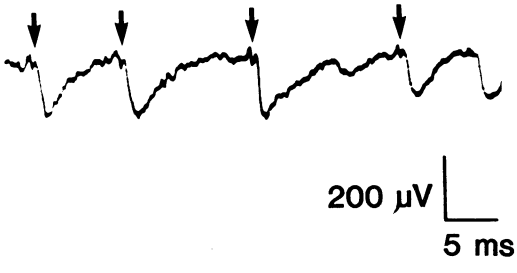

FIG. 1. Spontaneous juxtazonal potentials (JZPs), recorded just below the surface of the superior colliculus. Note the long duration of the JZPs and the small biphasic prepotentials (*arrows*) that preceded them. These potentials occurred in the absence of deliberate visual stimulation, but the animal was not paralyzed and some retinal slip may have resulted from drift in eye position.

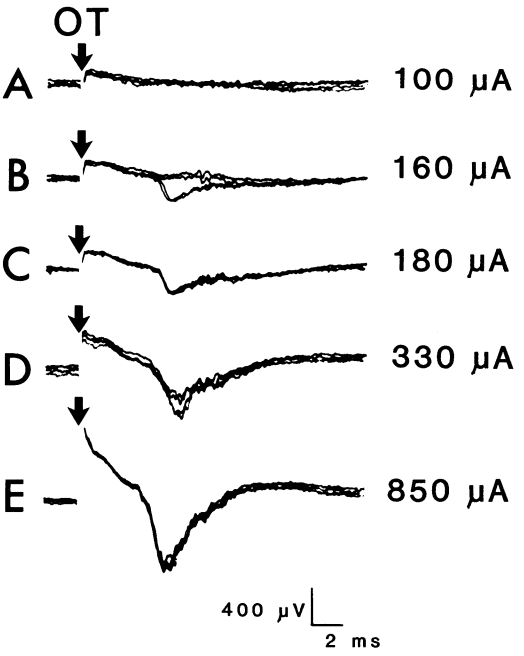

FIG. 2. All-or-none nature of electrically evoked juxtazonal potentials (JZPs) and their relation to the large negative field potential of the upper stratum griseum superficiale (SGS). In *B*, a unitary JZP was evoked in 2 of 4 superimposed records by near-threshold stimulation (*arrow*; 160 μA) of the optic tract (OT). Weaker shocks (*A*; 100 μA) never evoked the JZP, whereas stronger ones (*C*; 180 μA) invariably did so. Further increases in intensity (*D*; 330 μA) recruited a second, higher-threshold JZP, which occurred on 2 of the 4 superimposed records and can be seen riding on the lower-threshold JZP. With intense shocks to the OT (*E*; 850 μA), additional JZPs were recruited and summed to produce a large negative field potential. Four superimposed traces shown in each case. Stimulus duration was 50 μs for these and all other illustrated records.

Figure 2 illustrates the unitary nature of electrically evoked JZPs. In Fig. 2*B*, the stimulus to the optic tract (OT; arrow) was just at threshold for a single JZP, which appeared in two of the four superimposed traces. Note that the JZP was an all-or-none event having a fixed latency. The JZP also had a well-defined threshold. The slightly weaker OT shock in Fig. 2*A* failed to evoke the JZP,

presumably because it fell below the activation threshold of the W-cell axon triggering this JZP. Slightly stronger shocks (Fig. 2*C*) produced the JZP every time. Further increases in stimulus intensity recruited additional all-or-nonc JZPs (Fig. 2*D*) to yield at the highest intensities a large negative field potential (Fig. 2*E*).

Latency-difference estimates of conduction velocity of JZP-triggering axons

The conduction velocity of an axon responsible for a JZP can be estimated if the same JZP is evoked in isolation by shocks delivered to either of two sites along the optic pathway. The difference in the latency of the JZP when evoked from these two sites would reflect the time required for impulse conduction over the known distance between these sites. In practice, this latency-difference method was rarely applicable, because many JZPs could be evoked from each stimulus site (see Fig. 2), and the lowest-threshold JZP for one stimulus site almost never corresponded to that for another site. In two instances, however, the same JZP could be evoked in isolation from two stimulus sites, and the records of Figs. 3–6 illustrate the properties of one of these JZPs. This JZP was elicited from the OX with a latency of 8.3 ms and from the OT with a latency of 5.9 ms (Fig. 3). Dividing the difference in latency (2.4 ms) into the conduction distance between OX and OT (13.5 mm) yielded an estimated conduction velocity of 5.6 m/s for the axon triggering this JZP.

The validity of this conduction-velocity estimate hinges on certainty that the JZPs evoked from the two stimulus sites were the same. As shown in Fig. 3, the OX-evoked JZP appeared somewhat larger in amplitude than that evoked from the OT, but this discrepancy was largely attributable to the different base lines upon which they rode. More direct evidence that the JZPs were the same was obtained using a collision technique. Note that a suprathreshold shock to the more central of the two stimulus sites (the OT) must evoke not only the orthodromic spike, which triggers the JZP, but also an antidromic spike in the same axon. Until this antidromic spike passes by the more peripheral stimulus site (the OX), any orthodromic spike evoked by a suprathreshold shock to

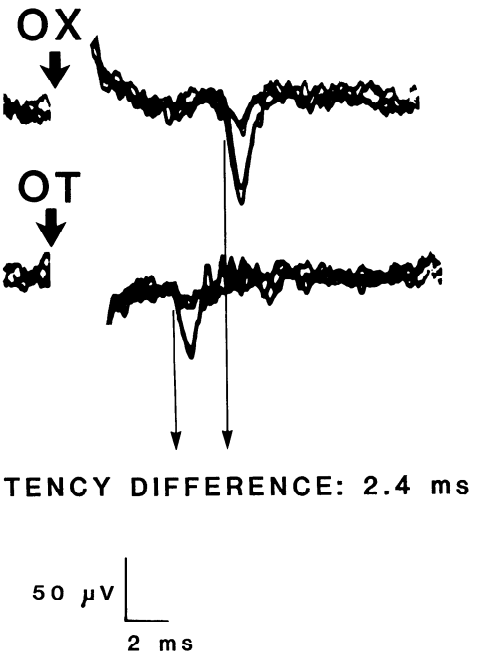

FIG. 3. A single unitary juxtazonal potential (JZP) that could be evoked in isolation from either of two stimulus sites in the optic pathway. The JZP occurred about half the time (and on 2 of 4 superimposed records illustrated) following near-threshold shocks delivered either to the optic chiasm (OX; 780 μA) or to the optic tract (OT; 530 μA). The latency of the JZP was 8.3 ms when evoked from the OX and 5.9 ms when evoked from the OT, yielding a latency difference of 2.4 ms.

the peripheral site will collide with the antidromic spike and will thus fail to generate a JZP. Thus, if the JZPs evoked from the OX and OT in Fig. 3 are triggered by the same axon, appropriate conditioning shocks to the OT should abolish JZPs evoked by suprathreshold OX shocks.

This prediction is confirmed in Fig. 4. In Fig. 4*A*, a suprathreshold shock to the OX evoked the JZP (arrow) every time. In Fig. 4*B*, the same OX shock was preceded by a conditioning stimulus to the OT; the OT stimulus was just at threshold for the JZP-triggering axon and evoked a JZP (asterisk) about half the time. Under these conditions, the JZP normally evoked by the OX shock (arrow) sometimes failed to occur. In Fig. 4*C*, the six superimposed records of Fig. 4*B* are shown individually. It is evident that the OX-evoked JZP (arrow) failed always, and only, when the OT shock exceeded the threshold of the axon triggering this JZP, as

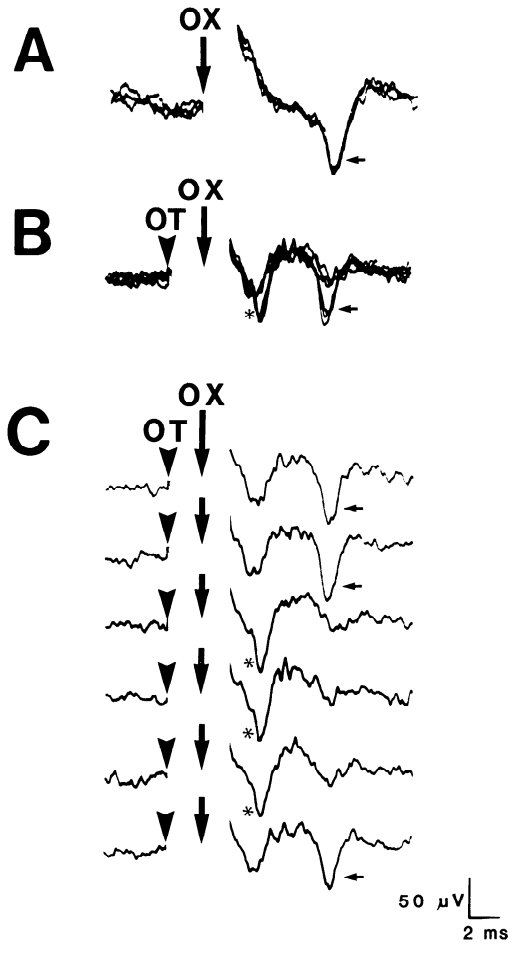

FIG. 4. Demonstration of a collision effect confirming that the juxtazonal potentials (JZPs) evoked from the optic chiasm (OX) and optic tract (OT) in Fig. 3 are the same. In *A*, a suprathreshold stimulus was delivered to the OX alone (*arrow*) and the JZP (*small arrow*) was evoked on each of the 3 superimposed records. In *B*, the same OX stimulus was preceded by a near-threshold stimulus to the OT, which evoked a JZP (*asterisk*) about half the time (3 of 6 superimposed records shown). Note the all-or-none nature of the OT-evoked JZP, which rode on an underlying negative potential (presumably a lower-threshold JZP or the sum of several such JZPs; cf. Fig. 2*D*). Under these conditions, the suprathreshold OX shock sometimes failed to evoke a JZP (*small arrow*). When the superimposed records of *B* are viewed individually (*C*), it is clear that the OX-evoked JZP (*small arrow*) failed always, and only, when the OT stimulus evoked a JZP (*asterisk*). This indicates that an antidromic spike, elicited whenever the OT shock exceeded the threshold of the JZP-triggering axon, collided with the OX-evoked orthodromic spike, which would otherwise have triggered its own JZP. Stimulus intensities: 780 (OX) and 560 μA (OT).

reflected by the occurrence of the OT-evoked JZP (asterisk). This confirms that the same axon mediated the JZPs evoked from the OX and OT in Figs. 3 and 4 and supports the validity of the latency-difference method used to estimate the conduction velocity of this axon.

A collision method for estimating conduction velocities of JZP-triggering axons

The collision effect just described can be used to generate a second, independent estimate of conduction velocity for the W-cell axon generating this same JZP. Note that there must be some critical interval between suprathreshold OT and OX shocks below which failure of the OX-evoked JZP will always occur and above which it never will. This critical interstimulus delay—the "collision interval"—represents the sum of the antidromic spike's conduction time from OT

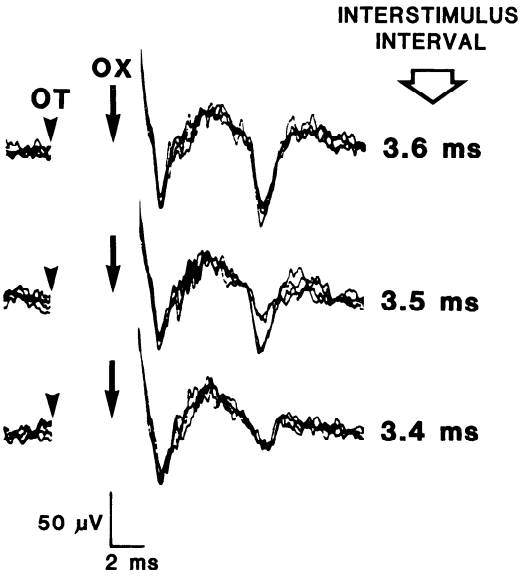

FIG. 5. Determination of the collision interval for the juxtazonal potential (JZP) illustrated in Figs. 3 and 4. A conditioning shock to the optic tract (OT) preceded a stimulus to the optic chiasm (OX) by various intervals; both the OT and OX shocks, when presented alone, were suprathreshold for the JZP. At an interstimulus interval of 3.6 ms (*top*), collision-induced failure of the OX-evoked JZP never occurred; at 3.4 ms (*bottom*) it always did. At an intermediate interstimulus interval of 3.5 ms (*middle*), the "collision interval," the OX-evoked JZP was abolished about half the time (2 of 4 superimposed traces shown). Stimulus intensities: 625 (OT) and 780 μA (OX).

to OX plus the axon's relative refractory period, that is, the period after the passage of the antidromic spike during which the OX shock fails to elicit an action potential. If the collision interval and refractory period can be measured, the conduction velocity of the JZP-triggering axon can be estimated as (conduction distance)/(collision interval − refractory period).

Figure 5 illustrates the determination of the collision interval for the JZP shown in Figs. 3 and 4. Suprathreshold shocks were delivered to the OT and OX. Each, when presented alone, evoked the JZP every time (not shown). When the OT shock preceded the OX stimulus, however, failure of the OX-evoked JZP could occur, depending on the interstimulus delay. Collision never occurred at an interstimulus interval of 3.6 ms (top panel), but always occurred at a slightly shorter interval of 3.4 ms (bottom). At an intermediate interval (3.5 ms, middle panel), collision occurred about half the time and in two of the four superimposed records shown. Note the all-or-none nature of collision-induced failure of the OX-evoked JZP. For the purposes of this study, the collision interval was defined as the interstimulus interval that resulted in collision roughly half the time, in this case, 3.5 ms. The measured collision interval was not dependent on the intensity of the suprathreshold OT shock.

In order to determine how much of the measured collision interval was attributable to the axon's relative refractory period, paired shocks to the OX were delivered at progressively smaller intervals until the JZP evoked by the second shock failed in an all-or-none manner to occur. The OX shocks were matched in intensity to those used to determine the collision interval (Fig. 5). As shown in Fig. 6, both OX shocks evoked JZPs at interstimulus intervals of 3.0, 2.0, and 1.2 ms (top three traces). The traces are aligned on the onset of the second stimulus, to show the slight delay of the second JZP at the shorter intervals. This was probably due to the period of subnormal conduction velocity that presumably followed the first spike (see Ref. 54 for review). At an interval of 1.0 ms, the second OX shock failed to trigger a JZP (bottom trace), presumably because it failed to overcome the relative refractoriness

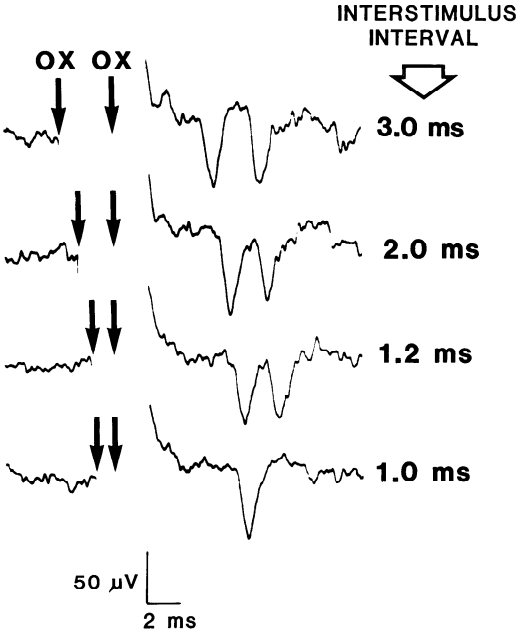

FIG. 6. Determination of the refractory period for the axon mediating the juxtazonal potential (JZP) illustrated in Figs. 3–5. Paired suprathreshold shocks were delivered to the optic chiasm (OX) at various intervals. The traces have been aligned on the onset of the second stimulus. At interstimulus intervals of 3.0, 2.0, and 1.2 ms (*top 3 traces*), both shocks evoked a JZP, though the second potential was delayed somewhat, presumably due to subnormal conduction velocity in the JZP-triggering axon following the passage of the first spike. When the shocks were separated by 1.0 ms (*bottom trace*), the second JZP failed to occur. The relative refractory period of the axon generating this JZP was taken to be the interval at which such paired shocks evoked the second JZP about half the time (1.1 ms, not shown). Shock intensity same as for Fig. 5.

of the JZP-mediating axon. This interpretation was supported by the finding that at interstimulus intervals at or just below 1.0 ms, the second JZP could be made to reemerge, simply by increasing the intensity of the OX shock. For the purposes of this study, the relative refractory period was defined as the interval at which the second JZP failed to occur about half the time; in this case, that interval was 1.1 ms (not shown).

For the JZP illustrated in Figs. 3–6, the collision interval was 3.5 ms (Fig. 5) and the refractory period was 1.1 ms (Fig. 6). Thus the conduction velocity of the axon triggering this JZP can be estimated as 13.5 mm/(3.5 ms − 1.1 ms) = 5.6 m/s. This cor-

responds precisely to the conduction velocity estimated for the same axon from the latency-difference measurements of Fig. 3. For the one other JZP that could be evoked in isolation from two sites (OD and OX), there was again good agreement between the axonal conduction-velocity estimates obtained by the latency-difference (3.9 m/s) and collision methods (4.2 m/s). Conduction-velocity estimates based on the collision method were essentially independent of the amount of current delivered to the peripheral stimulus

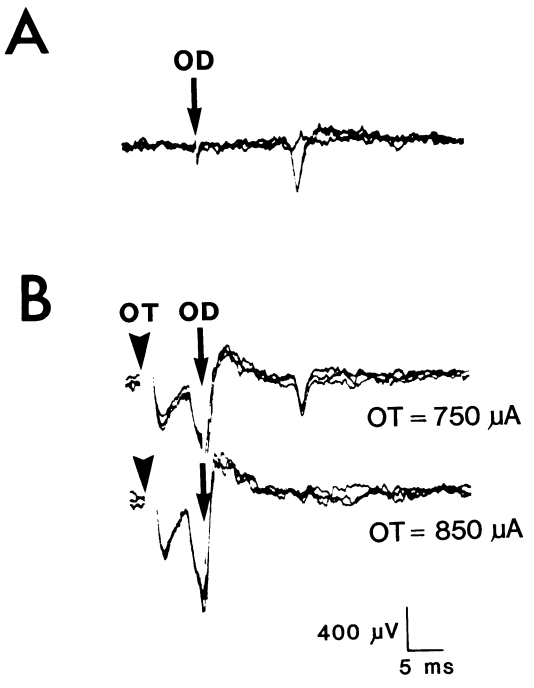

FIG. 7. Demonstration of the collision effect for a juxtazonal potential (JZP) that could be electrically evoked in isolation from only a single stimulus site—the optic disk (OD). *A*: near-threshold shock to the OD (300 μA) evoked the JZP in all-or-none fashion on two of three superimposed records shown. *B*: a suprathreshold OD stimulus (400 μA), which invariably evoked the JZP when presented alone, was preceded by a conditioning shock to the optic tract (OT). At an intensity of 750 μA, the OT shock had no apparent effect on the OD-evoked JZP, which occurred every time (*upper trace*). However, at slightly greater intensity (850 μA; lower trace), the OT shock abolished the OD-evoked JZP, through collision of antidromic and orthodromic spikes in the JZP-triggering axon. The large negative field potential evoked by the OT shock is visible immediately before the onset of the OD stimulus. Three superimposed records in each panel. Interstimulus interval in *B*: 8.0 ms.

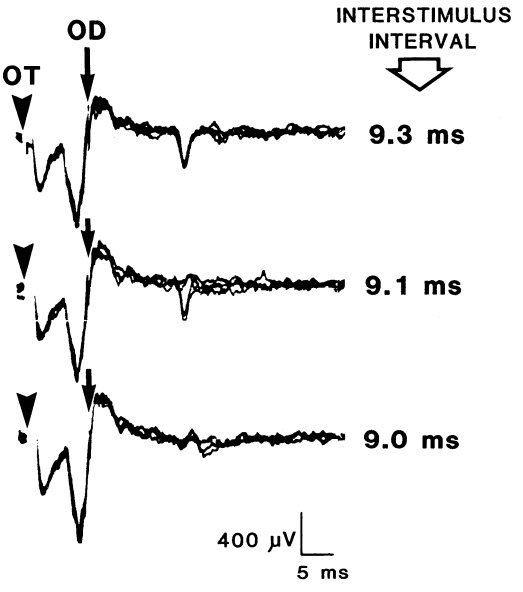

FIG. 8. Determination of the collision interval for the juxtazonal potential (JZP) illustrated in Fig. 7. A suprathreshold shock to the optic disk (OD; 400 μA) was preceded, at various intervals, by a conditioning shock to the optic tract (OT) that was suprathreshold for the collision effect demonstrated in Fig. 7 (900 μA). At an interstimulus interval of 9.1 ms (the collision interval) failure of the OD-evoked JZP occurred about half the time (*middle trace*). At longer interstimulus intervals (*top trace*) collision never occurred, whereas at shorter ones (*bottom trace*) it invariably did so. Four superimposed records in each trace.

site, since increases in shock intensity produced comparable reductions in measured collision interval and refractory period.

Generalization of the collision method

The latency-difference approach could be used only in those rare instances in which the same JZP could be evoked in isolation from two stimulus sites. By contrast, the collision method required only that a shock to one site evoke a JZP in isolation and that a shock to a second, more central, site elicit an antidromic spike in the axon triggering that JZP. It was of no consequence if the shock to the central site activated large numbers of axons, because only the antidromic spike in the JZP-triggering axon would affect the measured collision interval.

Figures 7 and 8 illustrate the use of the collision method to estimate the conduction velocity of an axon mediating a JZP that

could be evoked in isolation from only one stimulus site, the OD. As shown in Fig. 7*A*, near-threshold stimulation of the OD evoked this JZP in all-or-none fashion about half the time. For the records illustrated in Fig. 7*B*, the intensity of the OD stimulus was increased so that it invariably produced the JZP, and this OD shock was preceded by a strong conditioning shock to the OT. At an intensity of 750 μA (top trace), the conditioning shock had no apparent effect on the JZP, but a slightly stronger stimulus (850 μA; bottom trace) completely abolished the JZP. It is assumed that this resulted from collision of the OD-evoked orthodromic spike with an antidromic spike evoked by the OT shock in the axon triggering this JZP, an interpretation supported by the sharply defined threshold for the effect.

When the OT shock was suprathreshold for the collision effect, collision occurred about half the time at an interstimulus interval of 9.1 ms (Fig. 8, middle trace). This was taken as the collision interval. Collision never occurred at longer intervals (top trace) and invariably occurred at shorter ones (bottom trace). The axon's relative refractory period, determined by presenting paired shocks to the OD (not shown) and defined as the interstimulus interval at which the second JZP failed roughly half the time, was 1.5 ms. In these experiments, the stimulus used in the refractory period test was always matched to that used to determine the collision interval. The difference of the collision interval (9.1 ms) and the refractory period (1.5 ms) yields an estimated OD–OT conduction time of 7.6 ms. Dividing this value into the OD–OT electrode separation of 31.7 mm, determined by dissection, yields 4.2 m/s as an estimate of the conduction velocity of the axon triggering this JZP.

In some instances, JZPs evoked from the OD could be abolished by conditioning shocks delivered to either of the more central sites (OX or OT), permitting two largely independent conduction-velocity estimates to be made. This was true of the JZP just considered (Figs. 7 and 8). A conditioning shock to the OX produced failure of the JZP evoked by suprathreshold OD stimulation when the OX shock fell within the collision interval of 6.4 ms. As for conditioning shocks to the OT (Fig. 7), there was a sharp current threshold for evoking the collision effect from the OX. The estimated refractory period for the OD stimulus was 1.5 ms. Dividing the conduction distance between the OX and OD (19.2 mm) by the difference of the collision interval and refractory period yields an estimated conduction velocity of 3.9 m/s, which may be compared with the earlier estimate of 4.2 m/s for the same axon based on the OT–OD collision data. Such pairs of estimates could be made for nine JZP-triggering axons, and the discrepancies between the estimates were invariably small, ranging from 0.0 to 0.8 m/s (mean = 0.4 m/s).

Distribution of conduction velocities among JZP-triggering axons

Using the collision technique, conduction-velocity estimates were obtained for 31 axons triggering JZPs. As shown in Fig. 9, all of these axons were extremely slowly conducting, with an average conduction velocity (arrow) of 4.6 $\pm$ 1.0 m/s. The range of observed conduction velocities (2.9–6.8 m/s) fell entirely within the reported range for retinal W-cell axons, supporting earlier suggestions that W-cells project to the upper SGS of the cat's superior colliculus (7, 15, 18, 28). As will be discussed below, these results also indicate that W-cell afferents to the upper SGS are among the most slowly conducting of all W-cell axons.

Conduction-velocity estimates based on absolute latencies

Estimates of the conduction velocities of JZP-triggering axons were also obtained from the absolute latencies of individual evoked JZPs (Table 1). Note that the latency of an electrically evoked JZP reflects the sum of the total conduction time from stimulus site to colliculus plus the synaptic delay in the colliculus. By subtracting an estimate of the synaptic delay from the JZP's latency, one obtains an estimate of total conduction time. Dividing this value into the total conduction distance from stimulus site to colliculus provides an estimate of the *average* conduction velocity of the JZP-triggering axon, from the site of spike initiation to its terminals. In this way, estimates of average conduction velocity have been obtained for

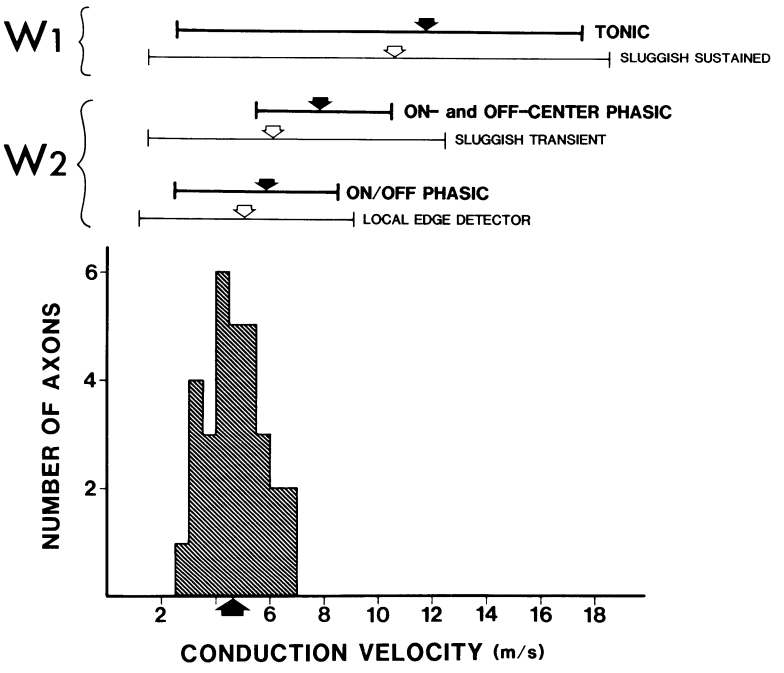

FIG. 9. Distribution of conduction velocities among 31 axons triggering juxtazonal potentials (JZPs) as estimated by the collision technique. In cases of multiple conduction-velocity estimates for individual axons, average values were used. The mean conduction velocity of JZP-triggering axons (*arrow*) was 4.6 m/s. The range (2.9–6.8 m/s) fell entirely within the reported range for retinal W-cell axons. The *bold lines* above show the ranges and mean (*arrow*) conduction velocites reported for 3 major receptive-field types of W-cells by Stone and Fukuda (49); *thin lines* represent data of Cleland and Levick (4, 5) for the corresponding receptive-field types. The conduction velocities of JZP-triggering axons corresponded closely in their range and mean to those of ON/OFF phasic W-cells (local edge detectors). There was also some overlap with the other distributions shown, but JZP-triggering axons appeared more slowly conducting than many of the ON- and OFF-center phasic cells and most of the tonic W-cells.

150 axons from the absolute latencies of JZPs evoked in all-or-none fashion from one of the three stimulus sites (Table 1). The synaptic delay was assumed to be 0.5 ms, a value that represents the average delay observed in these experiments between the presynaptically generated prepotential and postsynaptically mediated main component of JZPs (see also Ref. 28).

The mean conduction velocity of all JZP-triggering axons analyzed in this way was 3.5 ± 0.9 m/s (SD). This is somewhat slower than the mean conduction velocity of 4.6 m/s derived from the collision results. The same discrepancy is apparent when conduction-velocity estimates generated by the two methods are compared for the 31 individual axons analyzed by both techniques (Fig. 10). For nearly all of these axons (29/31), the absolute-latency method yielded a lower estimated conduction velocity than did the collision method.

This discrepancy is not unexpected. Retinal axons presumably undergo reductions in caliber, myelination, and conduction velocity as they enter the colliculus and ramify in the upper SGS. Slowing of impulse conduction in preterminal axonal branches would increase the latency of JZPs and reduce the axonal conduction velocities estimated directly from such latencies. By contrast, preterminal spike deceleration would have no effect on the measured collision interval, which is determined only by the segment of the axon lying between stimulus sites. If spike deceleration at the midbrain is responsible for the apparent underestimate of conduction velocity by the absolute-latency method, one would expect the effect to be most pronounced when the stimulus site is

TABLE 1. *Conduction-velocity estimates based on absolute latencies of individual JZPs*

	Stimulus Site		
	OT	OX	OD
	JZP latencies, ms		
Mean ± SD	5.8 ± 1.2	8.7 ± 2.3	14.2 ± 3.7
Range	3.3–8.2	5.8–16.5	9.0–28.2
	Estimated conduction velocities, m/s		
Mean ± SD	3.0 ± 0.9	3.6 ± 0.8	3.8 ± 0.9
Range	1.9–6.3	1.7–5.5	1.8–5.8
JZPs studied	33	57	60

Results for JZP latencies were lumped across collicular recording sites. Latencies at posterior recording sites tended to be longer, but substantially overlapped those encountered anteriorly. Location of recording sites did not differ as a function of stimulus site. JZP, juxtazonal potential; OT, optic tract; OX, optic chiasm; OD, optic disk.

near the colliculus, because in such cases the preterminal segment of the axon constitutes a relatively large proportion of the total path length. This is confirmed in Fig. 10, which shows that the discrepancy between absolute latency and collision estimates of conduction velocity is far greater for JZPs evoked from the OX (open circles) than for those driven from the OD (filled circles). Note also in Table 1 that absolute-latency estimates of conduction velocity are slowest, on average, for JZPs evoked from the OT and fastest when evoked from the OD.

The conduction velocity of JZP-triggering axons can also be inferred from the absolute-latency data of Table 1 in a way that circumvents any influence of the preterminal slowing just discussed. The difference between the mean absolute latency of JZPs evoked from two stimulus sites, divided into the mean conduction distance between those sites, yields an estimate of the mean conduc-

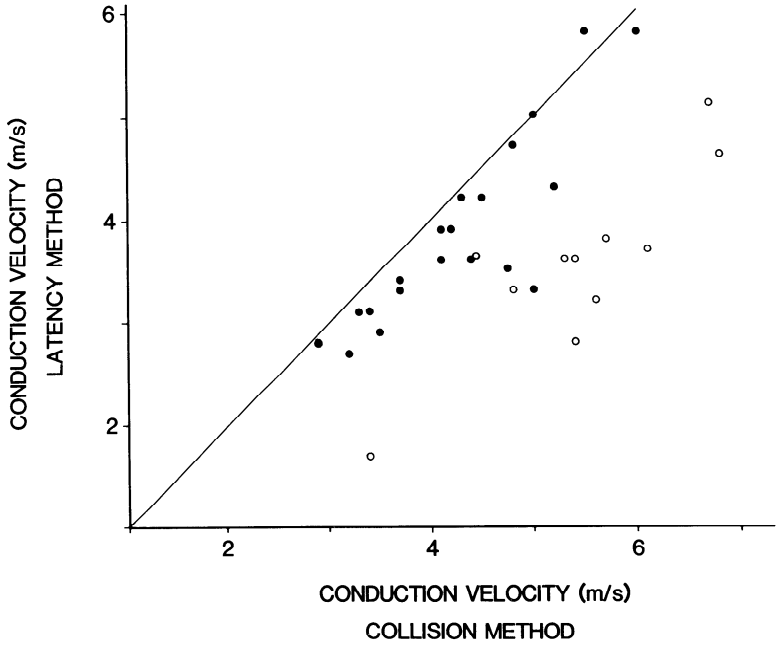

FIG. 10. Comparison for individual axons triggering juxtazonal potentials (JZPs) between conduction velocity estimate obtained by the collision method (*abscissa*) and that derived from the absolute latency of the JZP (*ordinate*). *Filled circles* represent cases in which the JZP was evoked in isolation from the optic disk and *open circles* those evoked from the optic chiasm. Axons for which the estimates corresponded perfectly would fall on the *straight line*. Note that the absolute-latency method yielded lower conduction-velocity estimates than did the collision method for nearly all axons and that the discrepancy was much more pronounced when the JZP was evoked from the chiasm than when evoked from the optic disk. Averaged values were used when more than one estimate was obtained for a single axon.

tion velocity of the axons triggering JZPs. The three estimates (OD–OX, OD–OT, OX–OT) that can be generated in this way ranged from 4.0 to 4.3 m/s, values that correspond closely to the estimate of 4.6 m/s based on the collision technique.

Conduction-velocity estimates based on latency of compound field potential

The large negative field potential evoked in the upper SGS by stimulation of retinal fibers represents the summation of many JZPs (Fig. 2 and Ref. 28). Thus the onset of this potential presumably reflects the action of the most rapidly conducting of the axons that mediate JZPs. A latency-difference analysis of the onset of the field potential will therefore define an upper bound for the conduction velocity of these axons. The latencies of onset of the field potential evoked from each of the three stimulus sites were determined for 11 collicular recording sites in four animals. For each pair of stimulus sites, the maximal conduction velocity of JZP-triggering axons was estimated as the difference in mean field-potential onset divided into the mean conduction distance separating these sites. Estimates ranged from 6.0 to 6.6 m/s, corresponding closely to the fastest conduction velocity obtained for any individual JZP-triggering axon by the collision method (6.8 m/s). Freeman and Singer (7), using a similar approach, estimated that retinal axons mediating the onset of this field potential conducted at velocities of 4–6 m/s.

Taken together, estimates of conduction velocity based on latency data for JZPs and their associated field potential support the conclusions drawn from the collision test that JZP-triggering axons conduct, on average, between 4 and 5 m/s and that few, if any, of these axons conduct as rapidly as 7 m/s.

DISCUSSION

The biophysical basis of the JZP remains to be established with certainty, but as reviewed in the INTRODUCTION, there is abundant evidence that this potential provides a reliable and convenient index of the activity of single W-cell afferents to the upper SGS. In this study, single electrically evoked JZPs have been used to estimate the conduction velocities of retinal afferents to the upper SGS by three separate approaches. That based on the absolute latency of evoked JZPs was the most straightforward, but the accuracy of this method appeared to be compromised by deceleration of action potentials as they enter the colliculus. A second approach, the latency-difference method, circumvented this limitation, but could seldom be implemented, since the same JZP could rarely be evoked in isolation from more than one stimulus site. For these reasons, the results of this study were obtained mainly from a third approach—the collision technique. A variety of observations indicate that the conduction-velocity estimates derived from this method reflect the properties of single axons. The collision was an all-or-none event (Figs. 4, 5, 7, 8). When both shocks were suprathreshold, collision occurred always and only when the interval between the stimuli was less than or equal to a critical value—the collision interval (Figs. 4, 8). When the shocks were presented at delays shorter than the collision interval, failure of the JZP occurred if, and only if, the conditioning shock exceeded a well-defined threshold that was presumably the threshold for activating the JZP-triggering axon (Fig. 7). This interpretation was confirmed directly for JZPs that could be activated in isolation from two sites, since failure occurred only when the conditioning stimulus itself evoked the JZP (Fig. 4).

Conduction-velocity estimates generated by the collision technique corresponded closely to those derived from other methods. When the latency-difference method could be applied (Fig. 3), it yielded a conduction-velocity estimate nearly identical to that derived for the same axon from collision data (Figs. 4–6). The mean conduction velocity of JZP-triggering axons, as inferred from the differences in mean JZP latency evoked from each of two sites, and the maximum conduction velocity among such axons, as inferred from differences in onset latency of the large field potential (this study and Ref. 7), closely matched estimates obtained by the collision technique. Even the absolute-latency method (Table 1), which may be biased toward lower conduction velocities due to intracollicular spike deceleration, yielded estimated conduction velocities only slightly

lower than those from the collision results (see also Ref. 28).

The present findings indicate that retinal axons triggering JZPs are among the most slowly conducting of all W-cell axons. As a class, W-cell axons have conduction velocities that range from roughly 1–20 m/s and average about 9 m/s (4, 5, 44, 49). As shown here, the axons of W-cells mediating JZPs conduct at 2.9–6.8 m/s with an average of 4.6 m/s. It is not certain that all retinal afferents to the upper SGS trigger JZPs, so the possibility of more rapidly conducting retinal input to this sublamina cannot be excluded. However, no such input is reflected in the field potentials of the upper SGS (7) or in the evoked responses of the vast majority of collicular neurons in the upper half of the superficial gray (in preparation). Thus the very slowly conducting W-cell afferents studied here are likely to constitute the main retinal input to the upper SGS.

W-cells innervating the upper SGS appear to differ from other W-cells not only in their axonal conduction velocities, but also in their pattern of decussation at the optic chiasm. Though many W-cells send axons into the ipsilateral optic tract (8, 23, 50), few of these axons reach the upper SGS, since retinal input to this sublayer is almost entirely crossed (1, 2, 10, 11, 14, 19, 28, 46). The crossed W-cell projection to the upper SGS originates in the temporal as well as the nasal hemiretina of the contralateral eye: the dense tier of retinal termination in the upper SGS extends to the extreme rostral pole of the colliculus, representing the ipsilateral visual hemifield (6, 10, 14).

A third distinguishing feature of the W-cells innervating the upper SGS appears to be their small soma size. Many of the smallest retinal ganglion cells are labeled after retrograde tracer deposits in the contralateral colliculus, but few, if any, can be labeled from the ipsilateral colliculus, or certain other known targets of W-cell projections, such as the C-laminae, medial interlaminar nucleus, or geniculate wing of the LGNd (27, 37, 44, 52, 53, 56). The crossed projection from the temporal retina to the anterior margin of the colliculus, which terminates primarily in the upper SGS (10, 14), arises almost exclusively from such extremely small ganglion cells (52, 53, 56). Taken together, these observations suggest that retinal input to the upper SGS comes predominantly from W-cells with very small somas, very slowly conducting axons, and crossed projections from the temporal retina.

Correlations between the receptive-field properties of W-cells and their soma size, conduction velocity, and decussation pattern (4, 5, 8, 16, 22, 23, 38, 44, 49, 50) prompted Rowe and Stone (39) to propose a formal division of the W-cell class into two subgroups. Their W1-cells tend to have sustained responses to standing contrast, small-to-medium size cell bodies, moderately slow conduction velocities (mean = 12 m/s), and uncrossed projections from the temporal retina. Receptive-field types included within this W1 subgroup are ON-center and OFF-center tonic, "suppressed by contrast," and color-coded W-cells.[1] Rowe and Stone's W2-cells tend to have transient light responses, very small somas, very slow conduction velocities (mean = 7 m/s), and crossed projections from the temporal retina. Their receptive fields are of the direction-selective, ON-center, OFF-center, or ON/OFF-center phasic types. The attributes of Rowe and Stone's W2-cells match those ascribed here to ganglion cells mediating the JZPs. Thus retinal input to the upper SGS probably originates mainly in phasic W-cells of the ON-center, OFF-center, ON/OFF-center, or direction-selective type.

Displayed in bold lines and labeling at the top of Fig. 9 are the ranges (horizontal bars) and mean conduction velocities (arrows) observed by Stone and Fukuda (49) for the most common receptive-field types within the W1 and W2 subgroups. Shown for comparison in finer lines and lettering are the findings of Cleland and Levick (4, 5) who used a different nomenclature for what appear to be the same receptive-field types.

---

[1] The receptive-field "types" used here are intended as useful and commonly accepted descriptive entities, rather than as rigid functional classes. Considerable debate exists over the best nomenclature and system of classification for ganglion cells other than X- or Y-cells (4, 5, 17, 35, 36, 39, 44, 47, 49, 51). In the interests of simplicity, I have adopted the scheme of Rowe, Stone, and colleagues for the discussion that follows.

Both sets of data were generated by a latency-difference analysis of antidromically activated ganglion cells. JZP-mediating W-cells clearly have slower axonal conduction velocities than the great majority of W1 cells with tonic, concentrically organized fields (sluggish-sustained cells), though the distributions overlap. There is a better match between JZP-triggering ganglion cells and the W2-cells shown, particularly those with ON/OFF-center phasic receptive fields (local edge detectors).

Conventional methods of receptive-field analysis cannot be applied to JZPs, since visual stimuli within the "response field" evoke multiple potentials (28). Nonetheless, the properties of this population response are consistent with mediation by one or more receptive-field types in the W2 subclass. All receptive-field types of this subclass prefer slow stimuli, give phasic responses to standing contrast, and, except for the ON-center direction-selective type (16, 49), have silent inhibitory surrounds. Similarly, JZPs are selective for slow stimulus velocities, respond phasically to stationary stimuli, and are poorly responsive to stimuli that extend beyond the response field (28). The JZP response field is ON/OFF in nature and lacks directional preference (28), suggesting an origin in ON/OFF center phasic W-cells, but convergence of ON- and OFF-center phasic cells and/or direction-selective neurons varying in preferred direction cannot be ruled out. On the other hand, limited latency-difference data (4, 5, 49) suggest that many ON- and OFF-center phasic and direction-selective W-cells have more rapidly conducting axons than any of the JZP-mediating ganglion cells of this study, whereas the ON/OFF phasic cells appear closely matched to JZP-triggering axons in conduction velocity (see Fig. 9). Absolute latencies of antidromic activation also support the view that ON/OFF phasic cells have among the most slowly conducting axons of W2-cells, though substantial overlap exists among the populations (4, 5, 22, 38, 49). Thus, on present evidence, the strongest candidates for input to the upper SGS appear to be the ON/OFF phasic W-cells, followed next by the ON- and OFF-center phasic and direction-selective types. A definitive functional characterization of the cell input to the upper SGS awaits more detailed study.

W-cell types other than those triggering JZPs almost certainly innervate the superior colliculus. All major W-cell receptive-field types have been antidromically activated from the midbrain (4, 5, 8, 49), and though some of these may have projected to the pretectum (16, 41) rather than the colliculus, there is ample independent confirmation of heterogeneity in the W-cell input to the colliculus itself. For example, some retinocollicular afferents, including most of those from the ipsilateral eye, terminate in the middle thickness of the SGS (sublayer II_2 of Ref. 19), in between the superficial current sink associated with the JZPs and the deeper one generated by retinal Y-cell input (1, 2, 10, 11, 14, 19, 30, 31, 45). A recent current source-density analysis has identified a small sink at this depth, which apparently reflects binocular input from W-cell axons conducting more rapidly than those triggering JZPs (~6–11 m/s). Retrograde tracer injections in the colliculus label small (non-alpha) ganglion cells in the ipsilateral temporal retina (52, 53, 56). These are presumably W-cells for the most part, but they are larger than those labeled in the contralateral temporal retina and presumably terminate deep to the upper SGS, which gets little ipsilateral input. Most W-cells antidromically activated from the ipsilateral midbrain have ON- or OFF-center tonic receptive fields (8). These observations suggest that the W-cells projecting to the middle thickness of the SGS have largely uncrossed projections from the temporal retina, as well as larger somata and more rapidly conducting axons than those of W-cells triggering the JZPs. These properties are characteristic of cells belonging to Rowe and Stone's W1 subgroup, raising the possibility that the deeper W-cell input may arise from ganglion cells with tonic, suppressed-by-contrast, and/or color-coded receptive fields (39).

The relative contributions of the various W-cell inputs to the receptive-field properties of collicular neurons remain to be determined, but preliminary indications are that the W2 input to the upper SGS is the more dominant. The upper SGS appears to contain, by far, the densest concentration of reti-

nal terminals of any layer (1, 2, 10, 11, 14, 19, 30, 31, 45, 46) and the current sink associated with this input is far larger than that associated with the deeper W-cell input, especially that from the ipsilateral eye (7). Ipsilaterally projecting W-cells probably account for <5% of all retinotectal terminals (2, 46). Preliminary results in an ongoing study indicate that the great majority of superficial collicular neurons are driven by W-cell axons conducting at the very slow velocities typical of JZP-triggering axons (in preparation). If more rapidly conducting W-cell input reaches these neurons, it is apparently insufficient to activate them under the conditions of these experiments.

The present evidence for a specialized W-cell input is but the latest in a series of findings distinguishing the upper SGS anatomically and functionally from the rest of the superficial gray. Besides its uniquely dense contralateral retinal input, the upper SGS is selectively targeted by input from the contralateral parabigeminal nucleus (9). The same sublayer is distinguished by its relatively high concentration of an endogenous opioid peptide (12) that appears to be contained within the processes of certain collicular interneurons (32). The cellular architecture and cortical inputs of the upper SGS also differ from those of the deeper parts of the superficial gray (21, 25, 42, 45, 55).

The functional significance of these connectional specializations of the upper SGS remains obscure. Inputs to the upper SGS seem likely to influence cells throughout the superficial laminae, since neurons at any depth in the superficial gray may extend dendritic processes into its upper tier (25, 45) and since most superficial collicular units seem to be driven by the very slowly conducting W-cell input that triggers JZPs (in preparation; see also Refs. 15, 28). Cells of the lower SGS are thus likely to integrate convergent inputs to the upper and lower superficial gray. On the other hand, neurons whose somas lie in the upper SGS have dendrites largely restricted to this sublayer (25, 45) and thus presumably receive their major synaptic inputs there. Since collicular cells projecting to the LGNd lie almost exclusively in the upper SGS (13, 20, 26), direct retinal influence on the tectogeniculate pathway probably originates predominantly in the subclass of W-cells innervating this collicular sublamina.

ACKNOWLEDGMENTS

I am grateful to Dr. James McIlwain for encouragement and valuable criticisms on the manuscript.

This work was supported by National Eye Institute Grant R01 EY-06108, Biomedical Research Support Grant PHS RR-05664-18, and a Trustee Grant from the Grass Foundation.

Received 27 February 1987; accepted in final form 8 June 1987.

REFERENCES

1. BEHAN, M. Identification and distribution of retinocollicular terminals in the cat: an electronmicroscopic autoradiographic study. *J. Comp. Neurol.* 199: 1–15, 1981.
2. BEHAN, M. A quantitative analysis of the ipsilateral retinocollicular projection in the cat: an EM degeneration and EM autoradiographic study. *J. Comp. Neurol.* 206: 253–258, 1982.
3. BEHAN, M. An EM-autoradiographic analysis of the projection from cortical areas 17, 18, and 19 to the superior colliculus in the cat. *J. Comp. Neurol.* 225: 591–604, 1984.
4. CLELAND, B. G. AND LEVICK, W. R. Brisk and sluggish concentrically organized ganglion cells in the cat's retina. *J. Physiol. Lond.* 240: 421–456, 1974.
5. CLELAND, B. G. AND LEVICK, W. R. Properties of rarely encountered types of ganglion cells in the cat's retina and an overall classification. *J. Physiol. Lond.* 240: 457–492, 1974.
6. FELDON, S., FELDON, P., AND KRUGER, L. Topography of the retinal projection upon the superior colliculus of the cat. *Vision Res.* 10: 135–143, 1970.
7. FREEMAN, B. AND SINGER, W. Direct and indirect visual inputs to superficial layers of cat superior colliculus: a current source-density analysis of electrically evoked potentials. *J. Neurophysiol.* 49: 1075–1091, 1983.
8. FUKUDA, Y. AND STONE, J. Retinal distribution and central projections of Y-, X-, and W-cells of the cat's retina. *J. Neurophysiol.* 37: 749–772, 1974.
9. GRAYBIEL, A. M. Satellite system of the superior colliculus: the parabigeminal nucleus and its projections to the superficial collicular layers. *Brain Res.* 145: 365–374, 1978.
10. GRAYBIEL, A. M. Anatomical organization of retinotectal afferents in the cat: an autoradiographic study. *Brain Res.* 96: 1–23, 1975.
11. GRAYBIEL, A. M. Evidence for banding of the cat's

ipsilateral retinotectal projection. *Brain Res.* 114: 318–327, 1976.
12. GRAYBIEL, A. M., BRECHA, N., AND KARTEN, H. J. Cluster-and-sheet pattern of enkephalin-like immunoreactivity in the superior colliculus of the cat. *Neuroscience* 12: 191–214, 1984.
13. HARRELL, J. V., CALDWELL, R. B., AND MIZE, R. R. The superior colliculus neurons which project to the dorsal and ventral lateral geniculate nuclei in the cat. *Exp. Brain Res.* 46: 234–242, 1982.
14. HARTING, J. K. AND GUILLERY, R. W. Organization of retinocollicular pathways in the cat. *J. Comp. Neurol.* 166: 133–144, 1976.
15. HOFFMANN, K.-P. Conduction velocity in pathways from retina to superior colliculus in the cat: a correlation with receptive-field properties. *J. Neurophysiol.* 36: 409–424, 1973.
16. HOFFMANN, K.-P. AND STONE, J. Retinal input to the nucleus of the optic tract of the cat assessed by antidromic activation of ganglion cells. *Exp. Brain Res.* 59: 395–403, 1985.
17. HUGHES, A. A rose by any other name . . . On 'Naming of Neurons' by Rowe and Stone. *Brain Behav. Evol.* 16: 52–64, 1979.
18. ITOH, K., CONLEY, M., AND DIAMOND, I. T. Different distributions of large and small ganglion cells in the cat after HRP injections of single layers of the lateral geniculate body and the superior colliculus. *Brain Res.* 207: 147–152, 1981.
19. KANASEKI, T. AND SPRAGUE, J. M. Anatomical organization of pretectal nuclei and tectal laminae in the cat. *J. Comp. Neurol.* 158: 319–338, 1974.
20. KAWAMURA, S., FUKUSHIMA, N., HATTORI, S., AND KUDO, M. Laminar segregation of cells of origin of ascending projections from the superficial layers of the superior colliculus. *Brain Res.* 184: 486–490, 1980.
21. KAWAMURA, S., SPRAGUE, J. M., AND NIIMI, K. Corticofugal projections from the visual cortices to the thalamus, pretectum and superior colliculus in the cat. *J. Comp. Neurol.* 158: 339–362, 1974.
22. KIRK, D. L., CLELAND, B. G., AND LEVICK, W. R. Axonal conduction latencies of cat retinal ganglion cells. *J. Neurophysiol.* 38: 1395–1402, 1975.
23. KIRK, D. L., LEVICK, W. R., AND CLELAND, B. G. The crossed or uncrossed destination of axons of sluggish-concentric and non-concentric cat retinal ganglion cells, with an overall synthesis of the visual field representation. *Vision Res.* 16: 233–236, 1976.
24. KOLB, H., NELSON, R., AND MARIANI, A. Amacrine cells, bipolar cells and ganglion cells of the cat retina: a Golgi study. *Vision Res.* 21: 1081–1114, 1981.
25. LANGER, T. P. *Cellular and Fiber Patterns in the Superior Colliculus of the Cat* (Ph.D. thesis). Seattle: University of Washington, 1976.
26. LANGER, T. P. AND COLBY, C. L. Subcortical projections to dorsal LGN. *Soc. Neurosci. Abstr.* 5: 792, 1979.
27. LEVENTHAL, A. G., RODIECK, R. W., AND DREHER, B. Central projections of cat retinal ganglion cells. *J. Comp. Neurol.* 237: 216–226, 1985.
28. MCILWAIN, J. T. Cat superior colliculus: Extracellular potentials related to W-cell synaptic actions. *J. Neurophysiol.* 41: 1343–1358, 1978.
29. MCILWAIN, J. T. AND LUFKIN, R. B. Distribution of direct Y-cell inputs to the cat's superior colliculus: are there spatial gradients? *Brain Res.* 103: 133–138, 1976.
30. MIZE, R. R. Patterns of convergence and divergence of retinal and cortical synaptic terminals in the cat superior colliculus. *Exp. Brain Res.* 51: 88–96, 1983.
31. MIZE, R. R. Variations in the retinal synapses of the cat superior colliculus revealed using quantitative electron microscope autoradiography. *Brain Res.* 269: 211–221, 1983.
32. MIZE, R. R. Colocalization of gamma-aminobutyric acid and leucine enkephalin in single neurons of the cat superior colliculus: an immunocytochemical study. *Soc. Neurosci. Abstr.* 12: 1033, 1986.
33. OGAWA, T. AND TAKAHASHI, Y. Retinotectal connectivities within the superficial layers of the cat's superior colliculus. *Brain Res.* 217: 1–11, 1981.
34. PALMER, L. A. AND ROSENQUIST, A. C. Visual receptive field of single striate cortical units projecting to the superior colliculus in the cat. *Brain Res.* 67: 27–42, 1974.
35. RODIECK, R. W. Visual pathways. *Annu. Rev. Neurosci.* 2: 193–225, 1979.
36. RODIECK, R. W. AND BRENING, R. K. Retinal ganglion cells: properties, types, genera, pathways and trans-species comparisons. *Brain Behav. Evol.* 23: 121–164, 1983.
37. ROWE, M. H. AND DREHER, B. Retinal W-cell projections to the medial interlaminar nucleus in the cat: implications for ganglion cell classification. *J. Comp. Neurol.* 204: 117–133, 1982.
38. ROWE, M. H. AND STONE, J. Conduction velocity groupings among axons of cat retinal ganglion cells, and their relationship to retinal topography. *Exp. Brain Res.* 25: 339–357, 1976.
39. ROWE, M. H. AND STONE, J. Naming of neurons: classification and naming of cat retinal ganglion cells. *Brain Behav. Evol.* 14: 185–216, 1977.
40. SAWAI, H., FUKUDA, Y., AND WAKAKUWA, K. Axonal projections of X-cells to the superior colliculus and to the nucleus of the optic tract in cats. *Brain Res.* 341: 1–6, 1985.
41. SCHOPPMANN, A. AND HOFFMANN, K.-P. A comparison of visual responses in two pretectal nuclei and in the superior colliculus of the cat. *Exp. Brain Res.* 35: 495–510, 1979.
42. SEGAL, R. L. AND BECKSTEAD, R. M. The lateral suprasylvian corticotectal projection in cats. *J. Comp. Neurol.* 225: 259–275, 1984.
43. SHERK, H. A comparison of visual-response properties in cat's parabigeminal nucleus and superior colliculus. *J. Neurophysiol.* 42: 1640–1655, 1979.
44. STANFORD, L. R. W-cells in the cat retina: correlated morphological and physiological evidence for two distinct classes. *J. Neurophysiol.* 57: 218–244, 1987.
45. STERLING, P. Receptive fields and synaptic organization of the superficial grey layer of the cat superior colliculus. *Vision Res. 3, Suppl.*: 309–328, 1971.
46. STERLING, P. Quantitative mapping with the electron microscope: retinal terminals in the superior colliculus. *Brain Res.* 54: 347–354, 1973.
47. STONE, J. *Parallel Processing in the Visual System.*

The Classification of Retinal Ganglion Cells and its Impact on the Neurobiology of Vision. New York: Plenum, 1983.

48. STONE, J. AND CLARKE, R. Correlation between soma size and dendritic morphology in cat retinal ganglion cells: evidence for further variation in the gamma-cell class. *J. Comp. Neurol.* 192: 211–217, 1980.
49. STONE, J. AND FUKUDA, Y. Properties of cat retinal ganglion cells: a comparison of W-cells with X- and Y-cells. *J. Neurophysiol.* 37: 722–748, 1974.
50. STONE, J. AND FUKUDA, Y. The nasotemporal division of the cat's retina examined in terms of the Y-, X- and W-cells. *J. Comp. Neurol.* 155: 377–394, 1974.
51. STONE, J. AND HOFFMAN, K.-P. Very slow-conducting ganglion cells in the cat's retina: a major new functional type? *Brain Res.* 43: 610–616, 1972.
52. STONE, J. AND KEENS, J. Distribution of small and medium-sized ganglion cells in the cat's retina. *J. Comp. Neurol.* 192: 235–246, 1980.
53. STONE, J., LEVENTHAL, A. G., WATSON, C. R. R., KEENS, J., AND CLARKE, R. Gradients between nasal and temporal areas of the cat retina in the properties of retinal ganglion cells. *J. Comp. Neurol.* 192: 219–233, 1980.
54. SWADLOW, H. A., KOCSIS, J. D., AND WAXMAN, S. G. Modulation of impulse conduction along the axonal tree. *Annu. Rev. Biophys. Bioeng.* 9: 143–179, 1980.
55. UPDYKE, B. V. Topographic organization of the projections from cortical areas 17, 18, and 19 onto the thalamus, pretectum, and superior colliculus in the cat. *J. Comp. Neurol.*173: 81–122, 1977.
56. WÄSSLE, H. AND ILLING, R.-B. The retinal projection to the superior colliculus in the cat: A quantitative study with HRP. *J. Comp. Neurol.* 190: 333–356, 1980.